



Crop-precipitation coupling drives deep soil desiccation-revival cycles in semiarid agroecosystems of Chinese Loess Plateau



Chenyun Bai^a, Sidra Sohail^a, XiaoDi Tang^a, HanYang Tian^a, Xiaoyang Han^{a,b,*}, Yuanjun Zhu^{a,b,*}, Jiangbo Qiao^{a,b}

^a State Key Laboratory of Soil and Water Conservation and Desertification Control, College of Soil and Water Conservation Science and Engineering (Institute of Soil and Water Conservation), Northwest A&F University, Yangling, Shaanxi 712100, China

^b University of Chinese Academy of Sciences, Beijing 100101, China

ARTICLE INFO

Keywords:

Soil desiccation index
Soil water recharge
Crop rotation system
Semi-arid agroecosystems

ABSTRACT

Precipitation-driven water scarcity imposes a critical constraint on sustainable development in the Chinese Loess Plateau, where the development of desiccated soil layers (DSLs) through persistent soil water deficits has emerged as a major ecological stressor. Although previous studies have extensively characterized the dynamics of DSLs in reforested ecosystems, the mechanisms underlying their formation in agroecosystems remain not fully elucidated. Soil water dynamics throughout 0–300 cm soil profiles under a winter wheat (*Triticum aestivum* L.)–winter wheat–spring maize (*Zea mays* L.) rotation system (2003–2022) were systematically investigated using high-resolution monitoring data. The Soil Desiccation Index (SDI) was employed to quantify desiccation severity and evaluate interactions between precipitation variability and cropping patterns. Key findings revealed four primary thematic takeaways: 1) Significant interannual fluctuations in soil water storage (SWS: 382.7–924.7 mm), with pronounced seasonal variability (minimum: 560.6 mm in June; maximum: 690.6 mm in October); 2) Drought memory effects dominated interannual dynamics – SDI exceeded 75 % during drought/post-drought years, sustaining strongly/extremely desiccated layers (>8 months), yet all DSLs fully recovered following ≥ 2 consecutive wet years. Non-desiccated layers dominated observations in wet (72 %), normal (65 %), and drought years (49 %), reflecting precipitation-dependent water availability. 3) Deep soil desiccation (>200 cm) showed heightened sensitivity to antecedent precipitation deficits, with SDI–precipitation correlations intensifying with depth ($r^2 = -0.21$ at 60–100 cm; -0.41 at 120–200 cm; -0.54 at 220–300 cm; $p < 0.01$). 4) Spring maize cultivation outperformed winter wheat in soil water retention, particularly during June–September. These findings reveal the intervention mechanisms of cropping pattern adjustments on soil water resilience, clarify the hysteresis response patterns of deep soil drying to precipitation deficits, and enhance the theoretical framework of soil water resilience in semiarid regions.

1. Introduction

Soil water plays a critical role in terrestrial water resource systems, underpinning global hydrological cycles while sustaining agricultural ecosystems (Denissen et al., 2022; Li et al., 2024; McColl et al., 2017). Meteorological parameters and cropping systems exert significant control over soil water dynamics (Anantha et al., 2023; Molenaar et al., 2024; Sigler et al., 2020), which subsequently regulate crop productivity (Harder et al., 2025; Liebhard et al., 2022). Understanding

spatiotemporal soil water variability in agricultural systems semi-arid agroecosystems for crop optimizing productivity and enhancing resource use efficiency, ultimately driving the development of sustainable agricultural methodologies that balance ecological stewardship with food security demands.

In the semi-arid agroecosystems of the Chinese Loess Plateau, deep vadose zones structurally constrain groundwater recharge to root zones, making precipitation the primary water source for croplands (Hou et al., 2018; Zhu et al., 2019). Observational studies confirm a linear

* Corresponding authors at: State Key Laboratory of Soil and Water Conservation and Desertification Control, College of Soil and Water Conservation Science and Engineering (Institute of Soil and Water Conservation), Northwest A&F University, Yangling, Shaanxi 712100, China.

E-mail addresses: baichenyun1996@163.com (C. Bai), Sidfatima65@gmail.com (S. Sohail), 15596829021@126.com (X. Tang), thy_961015@126.com (H. Tian), xyhan11@nwafu.edu.cn (X. Han), zhuyj@nwafu.edu.cn (Y. Zhu), jiangboqiao815@163.com (J. Qiao).

relationship between precipitation and soil water storage under unsaturated conditions (Chen et al., 2024). Intense rainfall events—occurring 3–4 times annually—are the primary mechanism for soil water replenishment (Wang et al., 2013), while precipitation anomalies are key drivers of drought (Bevacqua et al., 2024). The Plateau's substantial loess deposits (ranging from tens to hundreds of meters in thickness) result in delayed precipitation recharge and temporally asynchronous water dynamics across soil profiles. For instance, Zhang et al. (2017) documented precipitation infiltration to 7.2 m depth in loamy soils over a 52-year period, underscoring the requirement for extended observational studies to comprehensively characterize precipitation impacts on soil water dynamics (Guillod et al., 2015; Scott et al., 2017). However, labor-intensive soil water measurements (Liu et al., 2010) and limited long-term monitoring restrict most research to short-term precipitation effects, leaving the persistence of soil water under variable rainfall patterns poorly understood.

Prolonged soil water deficits lead to desiccation processes that generate desiccated soil layers (DSLs), which effectively decouple vertical hydrological connectivity (Jia et al., 2020; Lal et al., 2023; Yu et al., 2021). These DSLs significantly reduce precipitation infiltration rates, limit groundwater recharge capacity, degrade soil structural quality, and compromise the soil's reservoir function, ultimately leading to: (1) vegetation degradation, (2) decreased land productivity, and (3) impaired ecosystem services including carbon sequestration and hydrological regulation (Jia et al., 2017; Shao et al., 2016). On the Loess Plateau, prolonged low precipitation, high evapotranspiration, and anthropogenic disturbances have exacerbated DSLs thickening and spatial expansion, raising scientific concerns (Ge et al., 2024; Shao et al., 2023).

Research on DSLs formation have primarily investigated artificial plantations and perennial forage systems (Liu et al., 2024). For instance, soil desiccation severity correlates positively with *Platycladus orientalis* stand age (Li et al., 2023). Orchards deplete deep soil water more extensively than farmland, intensifying desiccation (Chen et al., 2022; Yang et al., 2020), while perennial forage crops extract water beyond 15 m, creating irrecoverable deficits (Ali et al., 2021; Ge et al., 2022). Farmlands are frequently employed as controls with assumed optimal water conditions, though this presumption requires critical re-examination. Rising food demand has intensified agricultural water use, worsening soil desiccation (Dile et al., 2013; Liu et al., 2010). Recent vegetation degradation on the Plateau has further reduced ecological and economic returns, driving large-scale farmland conversion (Tian et al., 2024). Additionally, as a core area of China's national ecological security barrier, the Loess Plateau is mandated by the National High-Standard Farmland Construction Plan (2021–2030) to improve the efficient utilization of water and soil resources. Thus, elucidating the causes, mechanisms, and recovery potential of farmland DSLs is vital for sustainable land management and regional ecological security.

By analyzing soil water datasets and meteorological records from Loess Plateau croplands under winter wheat-spring maize rotation systems during 2003–2022, hydrological years were classified into three categories (wet, normal, and drought) based on standardized precipitation indices. Three planting patterns were defined by crop types and seasonal schedules. The severity of DSLs was quantified, and the linkage among precipitation, planting patterns, and DSLs distribution was examined using the Soil Desiccation Index (SDI). The study objectives were to: (1) assessing how planting patterns and precipitation regulate farmland soil water, and (2) characterizing DSL persistence and occurrence patterns. It was hypothesized that farmland DSLs are transient and recoverable under adequate precipitation. Based on 20-year continuous soil water monitoring data from Chinese Loess Plateau, this study overcomes the limitations of short-term observations in assessing precipitation lag effects, and can elucidate the cumulative mechanisms and recovery dynamics of DSLs under multi-year wet-dry cycles.

2. Materials and methods

2.1. Study area

This study was conducted at the Changwu Agro-Ecosystem Experimental Station (CWA, 35°12' N, 107°40' E, 1200 m a.s.l.) of the Chinese Academy of Sciences, situated in the southern Loess Plateau. The region is characterized by a warm temperate semi-humid continental monsoon climate, the region exhibits an average annual temperature of 9.1°C and a frost-free period of 171 days. Annual precipitation averages 584 mm, unevenly distributed and concentrated predominantly between July and September. Groundwater tables range from 50 to 80 m below the surface, limiting crop water accessibility. The soils in this region are classified as Endocalcic Chernozem (Calcaric, Siltic) (IUSS Working Group WRB, 2022). The plow layer (0–20 cm) exhibits a soil porosity of 45.6 %, bulk density of 1.3 g·cm⁻³, soil organic matter content of 14.15 g·kg⁻¹, and total nitrogen content of 0.97 g·kg⁻¹ (Zhu and Cui, 2019). Dominant cereal crops include winter wheat, spring maize, and potatoes, with a prevalent winter wheat–spring maize rotation system (Liu et al., 2010). As a rainfed agricultural zone lacking irrigation infrastructure, crop production relies entirely on natural precipitation.

2.2. Sampling and measurement

A long-term field experiment was conducted on a winter wheat–winter wheat-spring maize rotation from September 2002 to December 2022 in the CWA Comprehensive experimental area (52 × 52 m). During these years, winter wheat was cultivated for 14 seasons, and spring maize for 6 seasons in total (Fig. 1). During the study period, soil samples were systematically collected by using a soil auger with an inner diameter of 4.5 cm, either at the end of even-numbered months or the beginning of odd-numbered months each year. Sampling was conducted to a depth of 300 cm. Samples were collected at 10 cm intervals from 0 to 100 cm and at 20 cm intervals from 100 to 300 cm. Soil samples were collected 6 times a year; each time, 20 soil layers were sampled, for a total of 120 soil samples annually. To ensure data reliability, soil samples were replicated twice. Fresh soil samples were stored in aluminum boxes and dried at a constant temperature of 105°C for 10 h to determine SWC. The soil desiccation evaluation method devised by Li et al. (2007) was used to calculate SDI (Conventional assessment metrics for soil water deficit rely solely on soil water content, whereas the SDI, through integrating soil water retention capacity and wilting point parameters, enables quantitative classification of desiccation risk levels across distinct soil textural classes). The degree of soil desiccation was categorized into six levels as outlined in Table 1. The corresponding DSLs are extremely DSL(DSL_{ex}), intense (DSL_{in}), severe DSL(DSL_{se}), moderate DSL(DSL_{mo}), mild DSL(DSL_{mi}), and no desiccation soil layers (DSL_{no}). The SDI was calculated by using the following:

$$SDI = \frac{SSM - SWC}{SSM - WN} * 100\% \quad (1)$$

Where SSM stands for Soil Stable Moisture (15.5 %), WN for Wilting Point (10.6 %), and SWC for Soil Water Content (%) (Zhang et al., 2019).

Meteorological data, including precipitation, solar radiation, and atmospheric temperature, were obtained from the meteorological station at CWA. Precipitation data from 1957 to 2022 were analyzed using the P-III frequency distribution curve. Based on the frequency and amount of precipitation ($Cv = 0.2$, $Cs/Cv = 2.5$), each year was categorized into three types: wet years (rainfall frequency below 25 %), normal years (rainfall frequency between 25 % and 75 %), and drought years (frequency above 75 %). Specifically, precipitation exceeding 641.3 mm was categorized as wet years; during normal years, precipitation ranged between 489.5 mm and 641.3 mm; years having less than 489.5 mm precipitation fell into the category of drought years (Fig. 2).

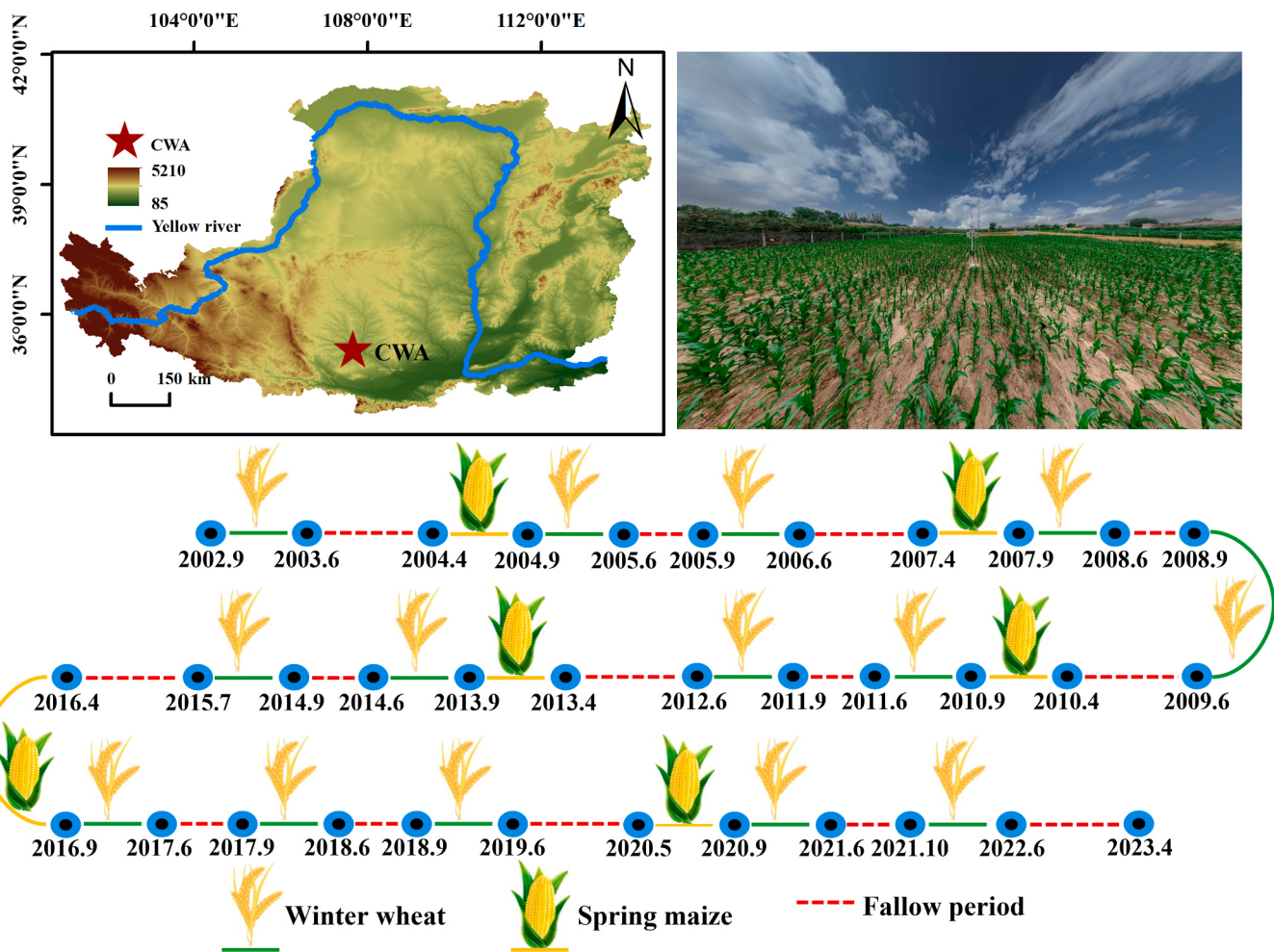


Fig. 1. Geographical location and site characteristics of farmland rotation systems in the loess plateau (2003–2023).

Table 1

Soil desiccation index(SDI) and the associated level of soil desiccation.

SDI(%)	SDI< 0	0 < SDI< 25	25 < SDI< 50	50 < SDI< 75	75 < SDI< 100	SDI> 100
Level of desiccation	No	Mild	Moderate	Severe	Intense	Extreme

Additionally, each year from 2002 to 2022 was classified into one of seven types based on the precipitation data and the preceding year's conditions, as depicted in Table 2.

2.3. Crop management

Winter wheat (var: ChangHan58) was sown in September and harvested in the following June, with a planting density of approximately 150 kg·ha⁻¹, a row spacing of 15 cm, and a seeding depth of 3 cm. Spring maize (var: DengHai3721) was sown in April and harvested in September, with a planting density of approximately 96,200 plants·ha⁻¹ and a seeding depth of 5 cm. Before sowing, basic fertilizers were applied, including urea (180 kg·ha⁻¹) and calcium superphosphate (120 kg·ha⁻¹). No additional fertilizers or irrigation were applied during the crop growing season. Weeding was done regularly, and other field management practices followed traditional farming methods in the region.

Planting patterns between 2003 and 2022 were classified into three types based on the crops grown and their planting schedules throughout the year: Pattern 1 (P1): winter wheat was planted from January to June, followed by fallow from July to December. P1 was observed in wet,

normal, and drought years. Pattern 2 (P2): the land remained fallow from January to March, followed by spring maize planting from April to September and winter wheat planting from September to December. P2 was observed only in normal years. Pattern 3 (P3): winter wheat was planted from January to June, fallowed in July and August, and then replanted with winter wheat from September to December. P3 was observed in wet and normal years.

2.4. Data processing and analysis

Owing to the lack of soil water data in December 2004 and December 2005, as well as the relatively low precipitation and temperature from early November to late February of the following year, combined with weak soil evaporation during this period, this study estimated the soil water content for December using data from October of the same year and February of the subsequent year. The surface soil horizon (0–50 cm) exhibited pronounced sensitivity to exogenous drivers including climatic variability and anthropogenic disturbances, and its dynamic changes in soil water are relatively complex. Therefore, this study did not analyze dynamic changes in soil surface water (0–50 cm).

The distribution of soil layers with varying degrees of dryness was

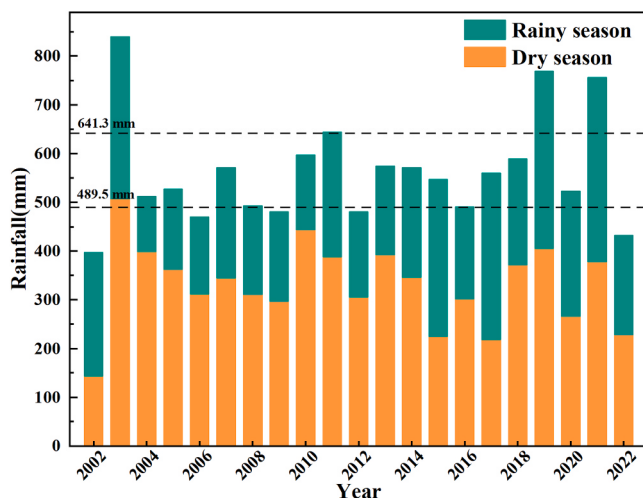


Fig. 2. Classification of years based on precipitation in the study area (2002–2022): < 489.5 mm as drought, > 641.3 mm as wet, and 489.5–641.3 mm as normal.

Table 2

Precipitation patterns and planting patterns for each year from 2003 to 2022. The abbreviations "W", "N", and "D" signify wet, normal, and drought years, with the letters before and after "-" indicating precipitation conditions of the preceding and current years.

Type	Wet years		Normal years			Drought years	
	N-W	D-W	W-N	N-N	D-N	W-D	N-D
P1	2019	2003		2015		2012	2006
						2022	2009
P2			2004	2016	2007		
			2020		2010		
					2013		
P3	2011			2005 2008			
	2021			2014 2017			
					2018		

analyzed by comparing their proportions to the total number of soil layers under different precipitation patterns and planting patterns. To minimize the influence of precipitation levels, the analysis focused solely on the effects of the three planting patterns under the N-N precipitation pattern on soil aridification.

This study utilized Microsoft Excel 2021 (Microsoft Corporation, Washington, USA) and SPSS 26.0 software (SPSS Corporation, Chicago, USA) for data organization and statistical analysis. Graphical visualizations were generated using OriginPro 2021 software (OriginLab Corporation, Massachusetts, USA) in conjunction with Microsoft Visio. Structural equation modeling (SEM) was conducted using IBM AMOS 26 software (SPSS Corporation, Chicago, USA) to identify the factors influencing SDI. The model incorporated meteorological variables, including precipitation, temperature, and net photosynthetically active radiation, along with crop-related parameters. Model fit was evaluated against established thresholds: $GFI/CFI/TLI > 0.90$, $RMSEA < 0.15$. Random Forest analysis was utilized to identify the key predictors of the SDI, considering meteorological factors and soil depth. Predictor importance was evaluated based on the percentage increase in mean squared error (MSE), with higher MSE% values indicating greater significance of the variable. The statistical significance of each predictor was further evaluated using the "rfPermute" package in R (Set ntree=1000 and 500 permutation tests).

3. Results

3.1. Dynamic changes of soil desiccation index

Over the 20-year observation period (2003–2022), soil water storage (SWS) in the 0–300 cm profile of rotational farmland displayed pronounced variability, with values spanning 382.7–924.7 mm. Annual averages fluctuated between 516.0 mm and 749.3 mm. A recurrent intra-annual hydrological cycle emerged, featuring sequential phases of depletion (January–June), replenishment (July–September), and secondary depletion (October–December). Minimum soil water storage (560.6 mm) occurred in June, contrasting with peak values (693.6 mm) in October post-monsoon. (Fig. 3).

Distinct interannual differences in soil desiccation, quantified by the SDI, were evident (Fig. 4). During 2004, 2005, 2016, 2019, and 2020, SDI values remained below 50 %, indicating moderate or slight desiccation. In contrast, during 2003, 2006, 2007, 2008, 2009, and 2010, SDI values in some soil layers exceeded 75 %, reflecting strong to extreme desiccation. These conditions persisted for over eight months each year, highlighting persistently low soil water levels. Between 2006 and 2011, DSLs extending deeper than 3 m were observed. Precipitation had a significant role in influencing soil desiccation dynamics. For instance, in June 2003, DSL_{ex} with SDI values exceeding 100 % were gradually alleviated by sustained precipitation, reducing the SDI below zero and fully restoring soil water in all desiccated layers.

3.2. Quantity distribution of DSLs

In normal and wet years, the proportions of DSL_{no} were 72 % and 65 %, respectively, which were considerably higher than the 49 % observed during drought years. In contrast, during drought years, the proportions of DSL_{mo} , DSL_{se} , DSL_{in} , and DSL_{ex} were 12 %, 10 %, 12 %, and 8 %, respectively, substantially exceeding those in wet years. Notably, during drought years, the proportion of DSL_{in} was 3.0 and 2.0 times higher than in normal and wet years, respectively, while the proportion of DSL_{ex} was 3.9 and 5.4 times higher than that in normal and wet years, respectively (Fig. 5a).

When the previous year was a wet year, DSL_{no} accounted for 87 % of the total, decreasing to 67 % in normal years and further to 43 % in drought years. Importantly, no DSL_{ex} were observed when the previous year was a wet year (Fig. 5b). Across different planting patterns, the proportions of DSL_{no} in P1, P2, and P3 were 78 %, 97 %, and 72 %, respectively. It is noteworthy that no DSL_{ex} were observed in P1, and only DSL_{mi} appeared in P2. In contrast, in P3, the proportions of DSL_{mo} , DSL_{se} , DSL_{in} , and DSL_{ex} were significantly higher than those in P1 and P2 (Fig. 5c).

3.3. Distribution of DSLs at different soil depth

Significant variations in soil desiccation depths were observed in rotational farmland under different annual precipitation patterns. During wet years, DSL_{ex} was observed at depths of 60–100 cm, accounting for 4 % of the total soil layers. During drought years, however, DSL_{ex} was more prominent, making up 9 % of soil layers at depths of 60–100 cm and 120–200 cm, and 4 % at 220–300 cm, which were the highest ratios recorded across all precipitation patterns. Moreover, in wet years, 68 % of the soil layers at 220–300 cm showed no signs of desiccation (Fig. 6a, d).

When the precipitation pattern differed from the previous year's but was consistent in the current year, the proportions of DSL_{no} within each soil depth range were influenced by the preceding year's precipitation pattern (W-N > N-N > D-N; W-D > N-D; N-W > D-W). Specifically, the differences in the proportions of DSL_{no} between W-N and D-N at depths of 60–100 cm, 120–200 cm, and 220–300 cm were 33 %, 52 %, and 82 %, respectively; between W-D and N-D they were 22 %, 58 %, and 72 %; and between N-W and D-W they were 17 %, 32 %, and 47 %,

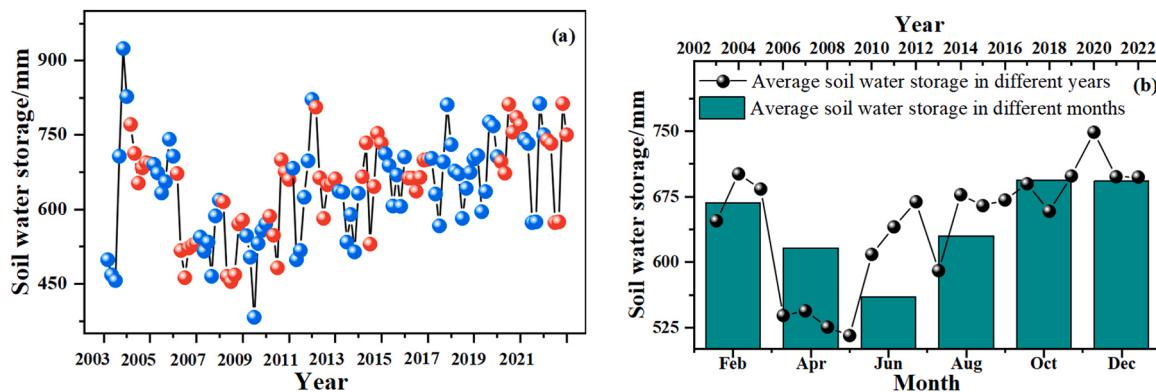


Fig. 3. Soil water storage dynamics (2003–2022, 0–300 cm): (a) monthly Distribution(different colors were used to distinguish adjacent years), (b) average across years and months.

respectively. These results indicated that as soil depth increased, the influence of the previous year's precipitation on soil desiccation intensified (Fig. 6b, e).

Different planting patterns also led to notable variations in soil desiccation. At depths of 60–100 cm, 120–200 cm, and 220–300 cm, the proportions of DSL_{no} in P2 were 97 %, 100 %, and 93 %, respectively, which were considerably higher than those in P1 and P3, indicating more favorable soil water conditions in P2. At depths of 120–200 cm and 220–300 cm, no DSL_{se} , DSL_{in} , or DSL_{ex} were present in P1, whereas P3 exhibited DSL_{ex} (Fig. 6c, f).

3.4. Distribution of DSLs in different months

Under different precipitation and planting patterns, the distribution of DSLs exhibited a consistent trend across different months: the proportion of DSL_{no} decreased from February to June and increased from June to December (except for P1), with the most severe soil desiccation observed in June. Specifically, in June, the proportions of DSL_{no} in wet, normal, and drought years were 27 %, 37 %, and 17 %, respectively. By December, these proportions had risen to 100 %, 90 %, and 63 %, respectively. The increases in these proportions from June to December were 73 %, 53 %, and 46 %, respectively, with the highest increase observed in wet years, followed by normal years, and the lowest in drought years. Moreover, when the precipitation year type remained constant, the precipitation pattern of the preceding year significantly affected the proportions of DSL_{no} . Particularly, following a wet year, the proportion of DSL_{no} from February to June was substantially higher than following a normal year, and after a normal year, this proportion was significantly higher than after a drought year. Among the three planting patterns, in June, August, and October, the proportions of DSL_{no} in P2 were 100 %, 100 %, and 97 %, respectively, which were markedly higher than those in P1 and P3. In October and December, P1 exhibited only DSL_{mi} , whereas P3 showed moderate to severe soil desiccation layers (Fig. 7)

3.5. Response characteristics of SDI to climatic factors and planting patterns

Random forest analysis revealed that all factors collectively explained 81.1 % of the variance in SDI (Fig. 8a). Among these factors, soil depth and rainfall were identified as the primary predictors of SDI, followed by monthly net radiation (MTR) and monthly average temperature (MAT). To further elucidate the effects of planting patterns and meteorological factors on SDI at various soil depths, structural equation modeling (SEM) was employed (Fig. 8a–d). Monthly precipitation (MP) exhibited a significant negative correlation with SDI ($P < 0.05$), and this correlation weakened with increasing soil depth. Conversely, annual precipitation (AP) had no significant effect on SDI in the 60–100 cm soil

layer but showed a significant negative correlation in the deeper layers of 120–200 cm and 220–300 cm ($P < 0.05$), with the correlation strengthening at greater depths. Similarly, the previous year's precipitation (PYP) was negatively associated with SDI, and this relationship intensified at deeper soil depths ($P < 0.05$). Both MAT and MTR had a positive influence on SDI. Although planting patterns showed a weak negative correlation with SDI, they exhibited a statistically significant relationship ($P < 0.05$). The SEM model explained 37–51 % of the variance in SDI and provided a good fit to the data (Fig. 8).

4. Discussion

4.1. DSLs are transient in farmland within the loess plateau region

This study systematically monitored soil water dynamics (0–300 cm depth) under a winter wheat-winter wheat-spring maize rotation system in the Loess Plateau Region during 2003–2022. The results demonstrated intermittent soil desiccation events, where DSLs persisted for > 5 years but showed gradual attenuation following wet years (Fig. 4). As a typical rain-fed agricultural region, soil water replenishment primarily depends on precipitation (Li et al., 2021). Following significant precipitation events, soil water is effectively replenished (White et al., 2019). For DSLs at the depths of 2–3 m, replenishment can take at least ten years, leading to the complete disappearance of soil drying phenomena (Liu et al., 2010). These findings suggest that DSLs in Loess Plateau farmlands exhibit temporal rather than permanent characteristics, consistent with Zhang et al. (2019). This alleviates concerns regarding permanent DSLs formation in regional agroecosystems (Huynh et al., 2024; Lal et al., 2023). However, some studies have reported the existence of permanent DSLs in farmland, potentially linked to climatic and soil conditions in different regions (Li, 1983). Given the uncertainties surrounding climate change, particularly its potential impacts on precipitation distribution and intensity (Ukkola et al., 2021), further research and continuous monitoring of soil water dynamics are crucial to ensure the long-term sustainability of farmland.

In the Chinese Loess Plateau Region, water consumption and precipitation recharge depth may exceed 300 cm in the farmland (Zhang et al., 2022). Cheng et al. (2021) used isotope fractionation methods to analyze the water use characteristics of winter wheat and revealed that the 300–400 cm soil layer contributes over 15 % of the water for winter wheat growth and development. Similarly, Q. Zhang et al. (2021) observed field data indicating that maize water consumption can reach depths of up to 420 cm. Our study's observations on wet-dry cycles in farmland at the 300 cm soil layer provide strong alignment with these observations. Nevertheless, some researchers argued that effectively replenishing soil water below 200 cm through precipitation remains challenging, emphasizing the need to focus on soil water dynamics within the upper 200 cm (Li et al., 2022; Wang et al., 2022; Yan Zhang

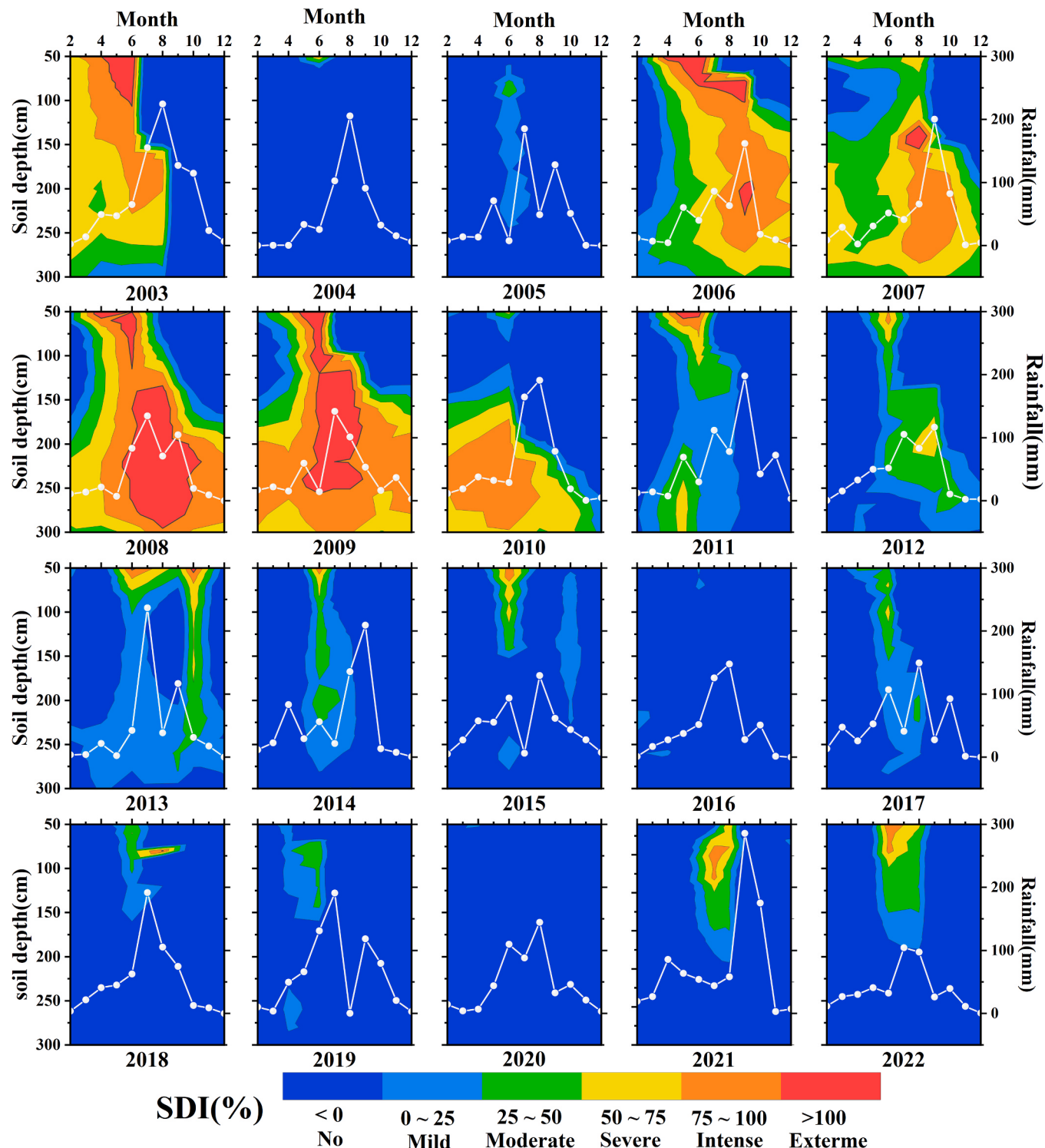


Fig. 4. Soil desiccation index (SDI) and Monthly precipitation, 2003–2022.

et al., 2022). This approach may underestimate changes in soil water storage, affecting the accuracy of evapotranspiration and water use efficiency calculations based on the water balance method. A deeper understanding of deep soil water storage mechanisms is essential for effective agricultural water resource management (Benettin et al., 2021). Deep soil water acts as a "soil reservoir," providing essential water support for crops and mitigating the adverse effects of drought on crop yields. Therefore, determining the depth of rainfall infiltration and adjusting cropping structures and farming practices based on crop water

requirements can enhance crop water use efficiency and optimize agricultural production strategies (Banihabib et al., 2018; Khattak et al., 2025). Accordingly, we recommend adopting various advanced methods and strategies in future research to increase monitoring depth, enabling a more comprehensive assessment of farmland water resources.

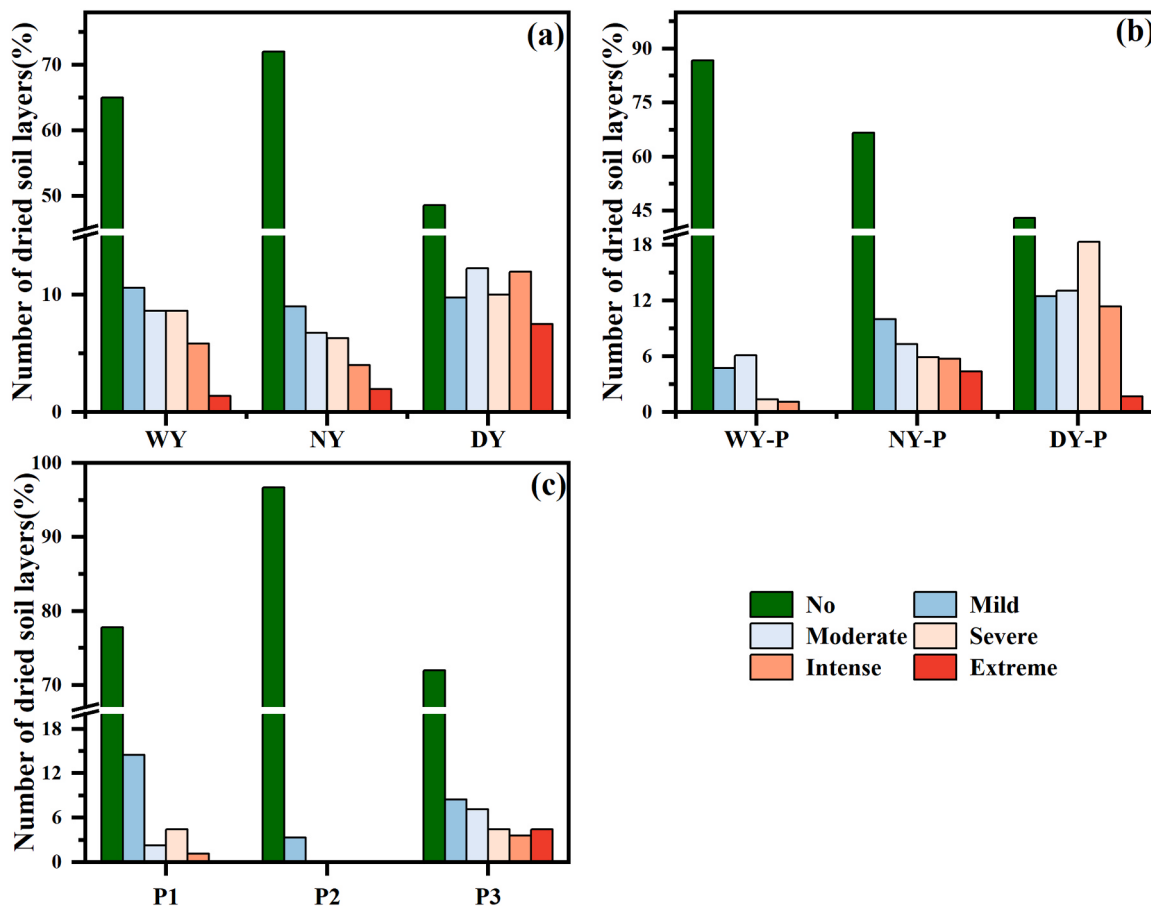


Fig. 5. Quantity distribution of DSLs: comparison across years (wet years (WY), normal years (NY), drought years (DY), the year preceding wet years (WY-P), normal years (NY-P), drought years (DY-P)) and Planting Modes (P1, P2, P3).

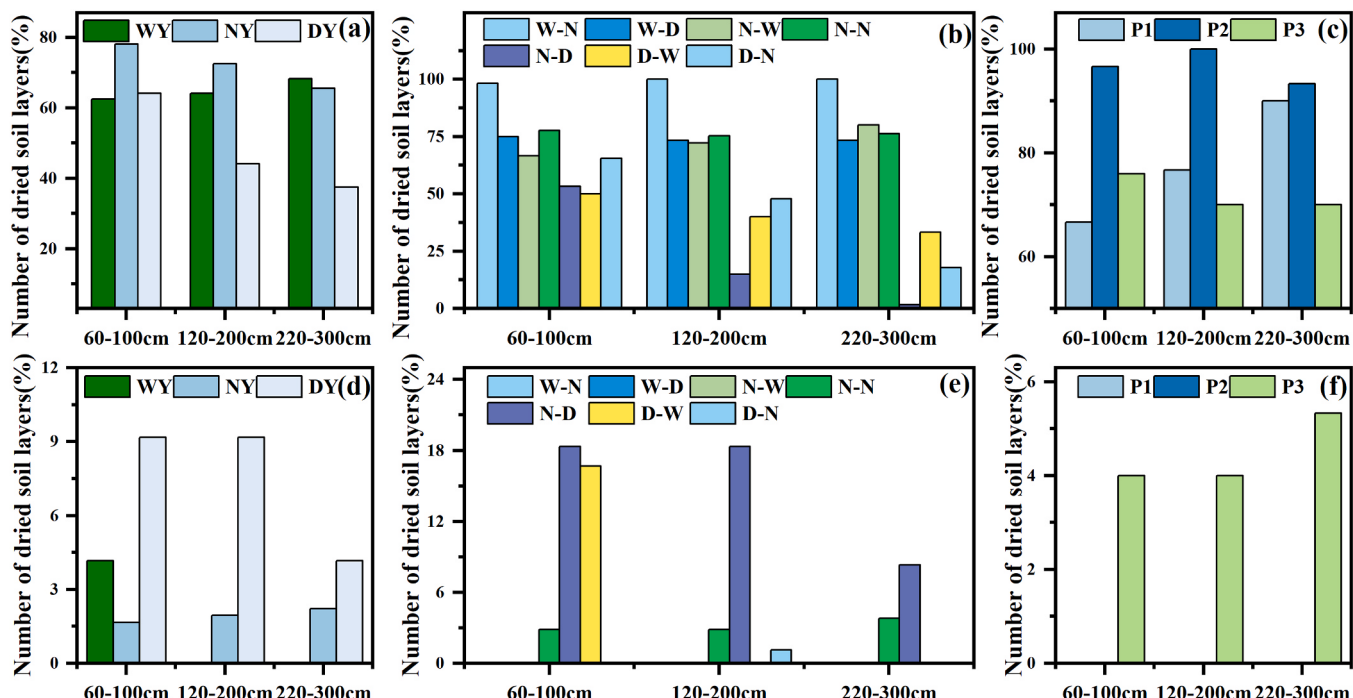


Fig. 6. Distribution characteristics of desiccated soil layers. (a-c) Non-desiccated layers; (d-f) extremely desiccated layers. Wy (Wet Year), NY (Normal Year), DY (Drought Year); in compound labels (e.g., W-N, W-D), the letters before/after the hyphen denote precipitation types of the preceding/current year (W: Wet, N: Normal, D: Drought).

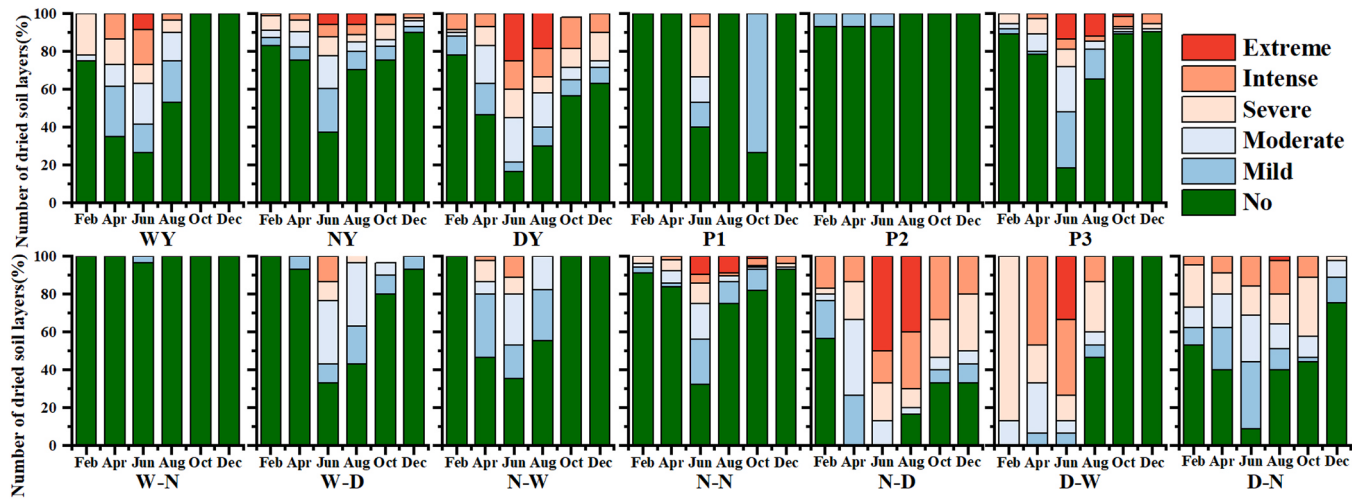


Fig. 7. Distribution of desiccated soil layers at different months. Wy (Wet Year), NY (Normal Year), DY (Drought Year); in compound labels (e.g., W-N, W-D), the letters before/after the hyphen denote precipitation types of the preceding/current year (W: Wet, N: Normal, D: Drought).

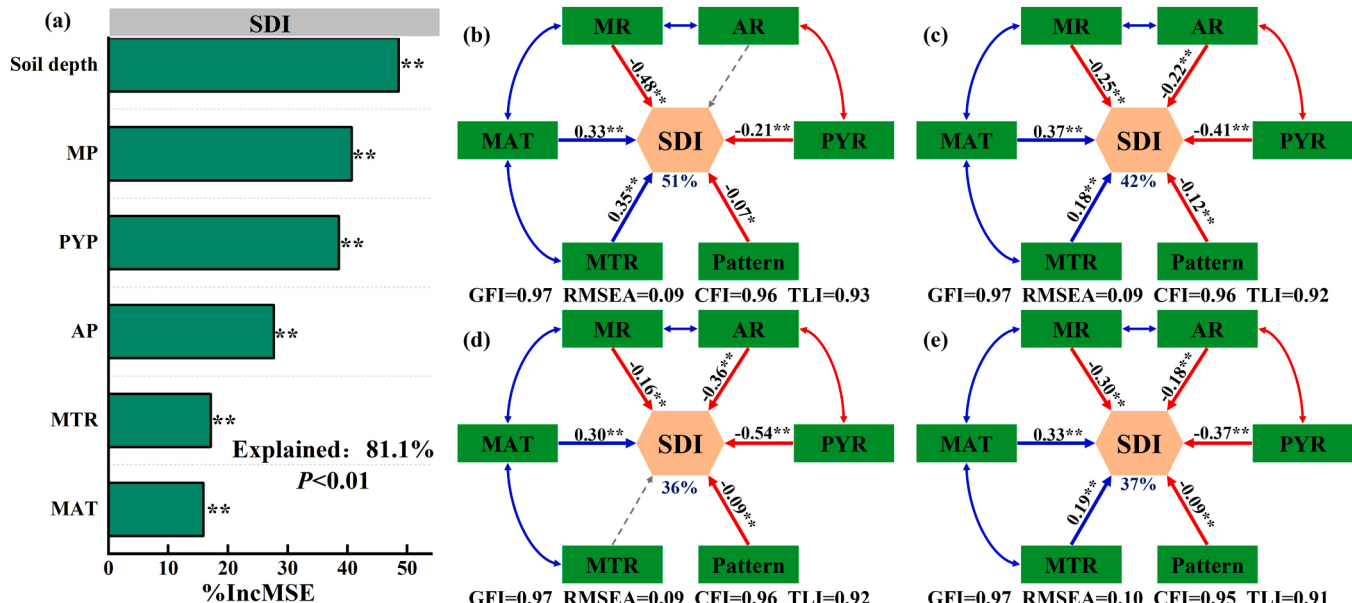


Fig. 8. Main predictors of soil desiccation index (SDI) and their influence across soil layers: (a) relative importance of soil depth and meteorological factors based on random forest analysis; (b–e) influence of environmental factors on SDI in different soil layers: (b) 60–100 cm, (c) 120–200 cm, (d) 220–300 cm, and (e) 60–300 cm. abbreviations: MP (monthly precipitation), AP (annual precipitation), PYP (previous year's precipitation), MAT (monthly average temperature), MTR (monthly total net radiation), pattern (planting patterns).

4.2. The relationship between precipitation patterns and soil desiccation

The Loess Plateau's deep soil profile (typically >3 m) and porous structure (bulk density 1.2–1.4 g/cm³) confer exceptional water retention capacity, enabling multi-year precipitation storage (Li et al., 2020; Zhao et al., 2017). Consequently, soil water regimes reflect the integrated effects of current and antecedent precipitation patterns (Hagen et al., 2020). Notably, precipitation from the previous year has a significant impact on soil desiccation, particularly in deeper soil layers, and exerts a stronger influence than current-year precipitation (Figs. 6 and 8). This phenomenon arises because current-year precipitation swiftly replenishes shallow soil water, while previous-year precipitation contributes to deep soil water through processes like infiltration and accumulation (Qiu et al., 2023; Xiang et al., 2020).

Soil water levels exhibit marked seasonal fluctuations, closely aligned with precipitation patterns. In this region, 40–75 % of annual

precipitation occurs during July–September (monsoon season), constituting the principal moisture source for soil recharge (Yu et al., 2021; R. Zhang et al., 2021). Consequently, soil water depletion before June is largely attributed to the stored precipitation from the previous year. Following June, with the arrival of current-year precipitation, soil water undergoes rapid replenishment (Zhu et al., 2021), predominantly relying on this year's precipitation. Notably, soil desiccation reaches its peak in June, aligning with our analytical results (Fig. 7).

The soil water dynamics of 2003 serve as a compelling case study (Fig. 4), illustrating the differential impacts of preceding and current-year precipitation on soil desiccation across various periods. In 2002 and 2003, the region experienced extreme drought and exceptionally wet conditions, with annual precipitation totals of 397 mm and 840 mm, respectively. Before June 2003, DSLs were prevalent within the 0–300 cm soil profile. However, substantial precipitation after June significantly replenished soil water, leading to the complete

disappearance of all DSLs. Additionally, compared to normal and drought years, wet years experienced higher precipitation levels during the rainy season, resulting in more pronounced soil water replenishment. Consequently, the period from June to December witnessed a more rapid increase in the proportion of DSL-free soil in wet years (Fig. 7).

4.3. The relationship between planting patterns and soil desiccation

Under the N-N precipitation patterns, the soil water conditions among the three planting patterns were ranked as P2 > P1 > P3. The critical divergence between P1 (fallow July–December) and P3 (winter wheat cultivation September–December) lies in vegetation cover duration—P3 maintains continuous crop coverage, whereas P1 allows post-harvest bare soil exposure. The reliance solely on rainfall for crop water supply in P3 leads to intensified soil water consumption due to crop growth, ultimately resulting in the poorest soil water conditions (Ge et al., 2020; Jia et al., 2017). In contrast, P2 exhibited the most favorable soil water conditions, likely attributable to the cultivation of spring maize from July to September. While maize consumes water during growth, its canopy acts as a natural 'sunshade', reducing direct sunlight exposure and thereby decreasing evaporation (Hakimi et al., 2018; Wang et al., 2011). Additionally, maize roots enhance soil aeration and permeability, facilitating water infiltration (Huang et al., 2017; Wu et al., 2022). As a result, the protective effect of surface vegetation cover in conserving soil water from July to September outweighs the water loss through plant transpiration. It is therefore recommended to implement post-harvest soil management practices during the critical July–September period following winter wheat harvest. These practices include stubble retention, straw mulching, and planting cover crops, collectively forming a protective barrier on the soil surface (Liao et al., 2025).

Field experiments have demonstrated that such interventions can reduce soil evaporation, enhance organic matter content, and improve water retention capacity compared to conventional tillage systems. This integrated approach directly addresses soil desiccation risks while promoting sustainable crop production through improved water use efficiency (WUE) and soil fertility. Overall, the winter wheat-spring maize rotation system in the Loess Plateau Region exhibits favorable soil water conditions and can be incorporated into the technical system of developing efficient dryland agriculture, as advocated by the Plan for Ecological Protection and High-quality Development of the Yellow River Basin. However, it is imperative to critically monitor soil water retention during years of extreme drought. Long-term data indicate that crop yields remain stable and relatively high under this rotation system, confirming its agroecological suitability. Nevertheless, caution is necessary to avoid introducing high-water-consuming crops, such as apple trees, for short-term economic benefits. Such practices could lead to the formation of permanent soil dry layers, irreversibly disrupting the ecological balance (Wang et al., 2024). However, due to limitations in monitoring depth and methodology, this study did not systematically characterize the dynamic characteristics of deep soil water below 3 m. Future research plans to combine deep-profile drilling sampling with long-term fixed-position observations to quantitatively analyze the spatiotemporal patterns of deep soil water. The methodology will also integrate double-ring infiltration experiments and hydrogen-oxygen isotope tracing technology to accurately delineate two critical hydrological processes: precipitation infiltration pathways and crop water sources in rotational farmland systems.

5. Conclusion

This study continuously monitored soil water content within the 0–300 cm soil layers of the winter wheat – winter wheat – spring maize rotation system in the Loess Plateau Region over a 20-year period (2003–2022) to comprehensively analyze the dynamic changes in soil

desiccation and its influencing factors. The main conclusions are as follows:

- (1) No permanent DSLs were detected in agricultural soils of the Loess Plateau Region during the 20-year observation period. Despite episodic soil desiccation events (SDI > 75 %) lasting ≤ 5 years, complete hydrological recovery was achieved following consecutive wet years
- (2) Multiannual precipitation regimes exerted significant control over DSL spatial-temporal dynamics, with lagged effects from antecedent precipitation. Soil desiccation was most severe during drought years, especially when the previous year was also a drought. Soil water was found to be at its worst in June and best in October.
- (3) Planting patterns exert a significant influence on soil water dynamics. Under the N-N precipitation pattern, spring maize cultivation exhibits more favorable soil water retention compared to winter wheat, particularly during the rainy season.

CRediT authorship contribution statement

Sidra Sohail: Writing – original draft, Conceptualization. **Chenyun Bai:** Writing – review & editing, Writing – original draft, Visualization, Methodology, Investigation, Formal analysis, Data curation. **HanYang Tian:** Writing – review & editing, Data curation. **XiaoDi Tang:** Validation, Methodology. **Yuanjun Zhu:** Supervision, Investigation, Data curation. **Jiangbo Qiao:** Project administration, Conceptualization. **Xiaoyang Han:** Writing – review & editing, Supervision, Funding acquisition, Conceptualization.

Declaration of Competing Interest

The authors declare that they have no known competing financial interests or personal relationships that could have appeared to influence the work reported in this paper.

Acknowledgments

This work was supported by the National Natural Science Foundation of China (42377316, 42307412, and 42007011) and the National Key R&D Program of China (2023YFD1900300).

Data availability

Data will be made available on request.

References

- Ali, G., Wang, Z., Li, X., Jin, N., Chu, H., Jing, L., 2021. Deep soil water deficit and recovery in alfalfa fields of the loess plateau of China. *Field Crops Res.* 260, 107990. <https://doi.org/10.1016/j.fcr.2020.107990>.
- Anantha, K., Garg, K.K., Akuraju, V., Sawargaonkar, G., Purushothaman, N.K., Sankar Das, B., Singh, R., Jat, M., 2023. Sustainable intensification opportunities for alfisols and vertisols landscape of the semi-arid tropics. *Agric. Water Manag.* 284, 108332. <https://doi.org/10.1016/j.agwat.2023.108332>.
- Banihabib, M.E., Vaziri, B., Javadi, S., 2018. A model for the assessment of the effect of mulching on aquifer recharging by rainfalls in an arid region. *J. Hydrol.* 567, 102–113. <https://doi.org/10.1016/j.jhydrol.2018.10.009>.
- Benettin, P., Nehemy, M.F., Asadollahi, M., Pratt, D., Bensimon, M., McDonnell, J.J., Rinaldo, A., 2021. Tracing and closing the water balance in a vegetated lysimeter. *Water Resour. Res.* 57, e2020WR029049. <https://doi.org/10.1029/2020WR029049>.
- Bevacqua, E., Rakovec, O., Schumacher, D.L., Kumar, R., Thober, S., Samaniego, L., Seneviratne, S.I., Zscheischler, J., 2024. Direct and lagged climate change effects intensified the 2022 european drought. *Nat. Geosci.* 17, 1100–1107. <https://doi.org/10.1038/s41561-024-01559-2>.
- Chen, M., Shao, M., Wei, X., Li, T., Shen, N., Mi, M., Zhao, C., Yang, X., Gan, M., Bai, X., Li, A., 2022. Response of the vertical distribution of soil water and nitrogen in the 5 m soil layer to the conversion of cropland to apple orchards in the loess plateau, China. *Agric. Ecosyst. Environ.* 333, 107960. <https://doi.org/10.1016/j.agee.2022.107960>.

- Chen, M., Yang, X., Zhang, X., Bai, Y., Shao, M., Wei, X., Jia, Y., Wang, Y., Jia, X., Zhu, Y., Zhang, Q., Zhu, X., Li, T., 2024. Response of soil water to long-term revegetation, topography, and precipitation on the Chinese loess plateau. *CATENA* 236, 107711. <https://doi.org/10.1016/j.catena.2023.107711>.
- Cheng, L., Qi, G., yanjiao, Li, Liu, W., 2021. Stable Isotope analysis of soil water utilization by winter wheat in dryland of loess tableland. *Res. Soil Water Conserv.* 170–176. <https://doi.org/10.13869/j.cnki.rswc.2021.03.020>.
- Denissen, J.M.C., Teuling, A.J., Pitman, A.J., Koiral, S., Migliavacca, M., Li, W., Reichstein, M., Winkler, A.J., Zhan, C., Orth, R., 2022. Widespread shift from ecosystem energy to water limitation with climate change. *Nat. Clim. Chang* 12, 677–684. <https://doi.org/10.1038/s41558-022-01403-8>.
- Dile, Y.T., Karlberg, L., Temesgen, M., Rockström, J., 2013. The role of water harvesting to achieve sustainable agricultural intensification and resilience against water related shocks in sub-Saharan Africa. *Agric. Ecosyst. Environ.* 181, 69–79. <https://doi.org/10.1016/j.agee.2013.09.014>.
- Ge, J., Fan, J., Yang, X., Luo, Z., Zhang, S., Yuan, H., 2022. Restoring soil water content after alfalfa and korshinsk psuehrash conversion to cropland and grassland. *Hydrol. Process.* 36, e14539. <https://doi.org/10.1002/hyp.14539>.
- Ge, J., Fan, J., Yuan, H., Yang, X., Jin, M., Wang, S., 2020. Soil water depletion and restoration under inter-conversion of food crop and alfalfa with three consecutive wet years. *J. Hydrol.* 585, 124851. <https://doi.org/10.1016/j.jhydrol.2020.124851>.
- Ge, D., Gao, X., Jiang, P., Li, B., He, N., Wu, Y., He, Q., Cai, Y., Li, C., Zhao, X., 2024. Deep soil desiccation hinders nitrate leaching to groundwater in the global largest apple cultivation area. *J. Hydrol.* 637, 131334. <https://doi.org/10.1016/j.jhydrol.2024.131334>.
- Guillod, B.P., Orłowsky, B., Miralles, D.G., Teuling, A.J., Seneviratne, S.I., 2015. Reconciling spatial and temporal soil moisture effects on afternoon rainfall. *Nat. Commun.* 6, 6443. <https://doi.org/10.1038/ncomms7443>.
- Hagen, K., Berger, A., Gartner, K., Geitner, C., Kofler, T., Kogelbauer, I., Kohl, B., Markart, G., Meißl, G., Niedertscheider, K., 2020. Event-based dynamics of the soil water content at alpine sites (Tyrol, Austria). *CATENA* 194, 104682. <https://doi.org/10.1016/j.catena.2020.104682>.
- Hakimi, L., Sadeghi, S.M.M., Van Stan, J.T., Pykner, T.G., Khosropour, E., 2018. Management of pomegranate (*Punica granatum*) orchards alters the supply and pathway of rain water reaching soils in an arid agricultural landscape. *Agric. Ecosyst. Environ.* 259, 77–85. <https://doi.org/10.1016/j.agee.2018.03.001>.
- Harder, P., Helgason, W.D., Johnson, B., Pomery, J.W., 2025. Observations and management implications of crop and water interactions in cold water-limited regions. *J. Hydrol.* 647, 132359. <https://doi.org/10.1016/j.jhydrol.2024.132359>.
- Hou, G., Bi, H., Wei, X., Kong, L., Wang, N., Zhou, Q., 2018. Response of soil moisture to Single-Rainfall events under three vegetation types in the gully region of the loess plateau. *Sustainability* 10, 3793. <https://doi.org/10.3390/su10103793>.
- Huang, Z., Tian, F.-P., Wu, G.-L., Liu, Y., Dang, Z.-Q., 2017. Legume grasslands promote precipitation infiltration better than gramineous grasslands in arid regions. *Land Degrad. Dev.* 28, 309–316. <https://doi.org/10.1002/lrd.2635>.
- Huynh, A., Aguirre, B.A., English, J., Guzman, D., Wright, A.J., 2024. Atmospheric drying and soil drying: differential effects on grass community composition. *Glob. Change Biol.* 30, e17106. <https://doi.org/10.1111/gcb.17106>.
- IUSS Working Group WRB, 2022. World Reference Base for Soil Resources. International soil classification system for naming soils and creating legends for soil maps, 4th edition. International Union of Soil Sciences (IUSS), Vienna, Austria.
- Jia, X., Shao, M., Zhu, Y., Luo, Y., 2017. Soil moisture decline due to afforestation across the loess plateau, China. *J. Hydrol.* 546, 113–122. <https://doi.org/10.1016/j.jhydrol.2017.01.011>.
- Jia, X., Zhao, C., Wang, Y., Zhu, Y., Wei, X., Shao, M., 2020. Traditional dry soil layer index method overestimates soil desiccation severity following conversion of cropland into forest and grassland on China's loess plateau. *Agric. Ecosyst. Environ.* 291, 106794. <https://doi.org/10.1016/j.agee.2019.106794>.
- Khattak, W.A., Sun, J., Zaman, F., Jalal, A., Shafiq, M., Manan, S., Hameed, R., Khan, I., Khan, I.U., Khan, K.A., Du, D., 2025. The role of agricultural land management in modulating water-carbon interplay within dryland ecological systems. *Agric. Ecosyst. Environ.* 378, 109315. <https://doi.org/10.1016/j.agee.2024.109315>.
- Lal, P., Shekhar, A., Gharun, M., Das, N.N., 2023. Spatiotemporal evolution of global long-term patterns of soil moisture. *Sci. Total Environ.* 867, 161470. <https://doi.org/10.1016/j.scitotenv.2023.161470>.
- Li, Y., 1983. The properties of water cycle in soil and their effect on water cycle for land in the loess region. *Acta Ecol. Sin.* 91, 101.
- Li, J., Chen, B., Li, X., Chen, J., Hao, M., 2007. Effects of deep soil desiccations on alfalfa grasslands in different rainfall areas of the loess plateau of China. *Acta Ecol. Sin.* 75–89.
- Li, B.-B., Li, P.-P., Zhang, W.-T., Ji, J.-Y., Liu, G.-B., Xu, M.-X., 2021. Deep soil moisture limits the sustainable vegetation restoration in arid and semi-arid loess plateau. *Geoderma* 399, 115122. <https://doi.org/10.1016/j.geoderma.2021.115122>.
- Li, L., Song, X., Feng, D., Li, H., Zhao, X., Meng, P., Fu, C., Wang, L., Jiao, R., Wei, W., Yang, N., Liu, Y., 2023. Impacts of climate change on soil desiccation in planted forests with different tree ages: a case study in the loess plateau of China. *Ecol. Indic.* 148, 110073. <https://doi.org/10.1016/j.ecolind.2023.110073>.
- Li, R., Wang, Y., Ji, W., Liu, W., Li, Z., 2024. Water deficit limits soil organic carbon sequestration under old apple orchards in the loess-covered region. *Agric. Ecosyst. Environ.* 359, 108739. <https://doi.org/10.1016/j.agee.2023.108739>.
- Li, M., Zhang, K., M. Eldoma, I., Fang, Y., Zhang, F., 2020. Plastic film mulching sustains high maize (*Zea mays L.*) grain yield and maintains soil water balance in semiarid environment. *Agronomy* 10, 600. <https://doi.org/10.3390/agronomy10040600>.
- Li, H., Zhang, Y., Sun, Y., Zhang, Q., Liu, P., Wang, X., Li, J., Wang, R., 2022. No-tillage with straw mulching improved grain yield by reducing soil water evaporation in the fallow period: a 12-year study on the loess plateau. *Soil Tillage Res.* 224, 105504. <https://doi.org/10.1016/j.still.2022.105504>.
- Liao, Y., Dong, L., Lv, W., Shi, J., Wu, J., Li, A., Zhang, H., Bai, R., Liu, Y., Li, J., Shangguan, Z., Deng, L., 2025. Response of soil infiltration and water to orchard mulching practices in the loess plateau, China. *CATENA* 252, 108848. <https://doi.org/10.1016/j.catena.2025.108848>.
- Liebhard, G., Klik, A., Neugschwandtner, R.W., Nolz, R., 2022. Effects of tillage systems on soil water distribution, crop development, and evaporation and transpiration rates of soybean. *Agric. Water Manag.* 269, 107719. <https://doi.org/10.1016/j.agwat.2022.107719>.
- Liu, X., Cai, L., Li, M., Yan, Y., Chen, H., Wang, F., 2024. Why does afforestation policy lead to a drying trend in soil moisture on the loess plateau? *Sci. Total Environ.* 953, 175912. <https://doi.org/10.1016/j.scitotenv.2024.175912>.
- Liu, W., Zhang, X.-C., Dang, T., Ouyang, Z., Li, Z., Wang, J., Wang, R., Gao, C., 2010. Soil water dynamics and deep soil recharge in a record wet year in the Southern loess plateau of China. *Agric. Water Manag.* 97, 1133–1138. <https://doi.org/10.1016/j.agwat.2010.01.001>.
- McColl, K.A., Aleemohammad, S.H., Akbar, R., Konings, A.G., Yueh, S., Entekhabi, D., 2017. The global distribution and dynamics of surface soil moisture. *Nat. Geosci.* 10, 100–104. <https://doi.org/10.1038/NGEO2868>.
- Molenaar, R.E., Kleidorfer, M., Kohl, B., Teuling, A.J., Achleitner, S., 2024. Does afforestation increase soil water buffering? A demonstrator study on soil moisture variability in the alpine geroldsbach catchment, Austria. *J. Hydrol.* 643, 131984. <https://doi.org/10.1016/j.jhydrol.2024.131984>.
- Qiu, D., Xu, R., Wu, C., Mu, X., Zhao, G., Gao, P., 2023. Effects of vegetation restoration on soil infiltrability and preferential flow in hilly gully areas of the loess plateau, China. *CATENA* 221, 106770. <https://doi.org/10.1016/j.catena.2022.106770>.
- Scott, C.P., Lohman, R.B., Jordan, T.E., 2017. InSAR constraints on soil moisture evolution after the March 2015 extreme precipitation event in Chile. *Sci. Rep.* 7, 4903. <https://doi.org/10.1038/s41598-017-05123-4>.
- Shao, X., Gao, X., Zeng, Y., Yang, M., Wang, Y., Zhao, X., 2023. Eco-Physiological constraints of deep soil desiccation in semiarid tree plantations. *Water Resour. Res.* 59, e2022WR034246. <https://doi.org/10.1029/2022WR034246>.
- Shao, M., Jia, X., Wang, Y., Zhu, Y., 2016. A review of studies on dried soil layers in the loess plateau. *Adv. Earth Sci.* 31, 14–22.
- Sigler, W.A., Ewing, S.A., Jones, C.A., Payn, R.A., Miller, P., Maneta, M., 2020. Water and nitrate loss from dryland agricultural soils is controlled by management, soils, and weather. *Agric. Ecosyst. Environ.* 304, 107158. <https://doi.org/10.1016/j.agee.2020.107158>.
- Tian, H., Jin, M., Sohail, S., Ma, C., Bai, C., Qiao, J., Han, X., Shao, M., 2024. The trade-off between soil water recovery and nitrate leaching following the orchard-to-cropland conversion in the Chinese loess plateau. *Sci. Rep.* 14, 29781. <https://doi.org/10.1038/s41598-024-80192-w>.
- Ukkola, A.M., De Kauwe, M.G., Roderick, M.L., Burrell, A., Lehmann, P., Pitman, A.J., 2021. Annual precipitation explains variability in dryland vegetation greenness globally but not locally. *Glob. Change Biol.* 27, 4367–4380. <https://doi.org/10.1111/gcb.15729>.
- Wang, H., Fan, J., Fu, W., Du, M., Zhou, G., Zhou, M., Hao, M., Shao, M., 2022. Good harvests of winter wheat from stored soil water and improved temperature during fallow period by plastic film mulching. *Agric. Water Manag.* 274, 107910. <https://doi.org/10.1016/j.agwat.2022.107910>.
- Wang, S., Fu, B., Gao, G., Liu, Y., Zhou, J., 2013. Responses of soil moisture in different land cover types to rainfall events in a re-vegetation catchment area of the loess plateau, China. *CATENA* 101, 122–128. <https://doi.org/10.1016/j.catena.2012.10.006>.
- Wang, X.C., Muhammad, T.N., Hao, M.D., Li, J., 2011. Sustainable recovery of soil desiccation in semi-humid region on the loess plateau. *Agric. Water Manag.* 98, 1262–1270. <https://doi.org/10.1016/j.agwat.2011.03.007>.
- Wang, S., Yang, M., Gao, X., Li, B., Cai, Y., Li, C., He, H., Zhao, X., 2024. Ecohydrological response to deep soil desiccation in a semiarid apple orchard. *Agric. For. Meteorol.* 354, 110089. <https://doi.org/10.1016/j.agrformet.2024.110089>.
- White, J., Berg, A.A., Champagne, C., Warland, J., Zhang, Y., 2019. Canola yield sensitivity to climate indicators and passive microwave-derived soil moisture estimates in Saskatchewan, Canada. *Agric. For. Meteorol.* 268, 354–362. <https://doi.org/10.1016/j.agrformet.2019.01.004>.
- Wu, X., Dang, X., Meng, Z., Fu, D., Cong, W., Zhao, F., Guo, J., 2022. Mechanisms of grazing management impact on preferential water flow and infiltration patterns in a semi-arid grassland in Northern China. *Sci. Total Environ.* 813, 152082. <https://doi.org/10.1016/j.scitotenv.2021.152082>.
- Xiang, W., Evaristo, J., Li, Z., 2020. Recharge mechanisms of deep soil water revealed by water isotopes in deep loess deposits. *Geoderma* 369, 114321. <https://doi.org/10.1016/j.geoderma.2020.114321>.
- Yang, M., Wang, S., Zhao, X., Gao, X., Liu, S., 2020. Soil properties of apple orchards on China's loess plateau. *Sci. Total Environ.* 723, 138041. <https://doi.org/10.1016/j.scitotenv.2020.138041>.
- Yu, S., Khan, S., Mo, F., Ren, A., Lin, W., Feng, Y., Dong, S., Ren, J., Wang, W., Noor, H., Yang, Z., Sun, M., Gao, Z., 2021. Determining optimal nitrogen input rate on the base of fallow season precipitation to achieve higher crop water productivity and yield. *Agric. Water Manag.* 246, 106689. <https://doi.org/10.1016/j.agwat.2020.106689>.
- Zhang, Yan, Dong, X., Yang, X., Munyampirwa, T., Shen, Y., 2022. The lagging movement of soil nitrate in comparison to that of soil water in the 500-cm soil profile. *Agric. Ecosyst. Environ.* 326, 107811. <https://doi.org/10.1016/j.agee.2021.107811>.
- Zhang, Z.Q., Evaristo, J., Li, Z., Si, B.C., McDonnell, J.J., 2017. Tritium analysis shows apple trees May be transpiring water several decades old. *Hydrol. Process.* 31, 1196–1201. <https://doi.org/10.1002/hyp.11108>.

- Zhang, R., Li, Z., Wang, L., 2019. Relationship between soil moisture dynamics, crop growth and precipitation in rain-fed area of the loess Tableland, China. *Chin. J. Appl. Ecol.* 359, 369. <https://doi.org/10.13287/j.1001-9332.201902.015>.
- Zhang, Yuanhong, Li, H., Sun, Y., Zhang, Q., Liu, P., Wang, R., Li, J., 2022. Temporal stability analysis evaluates soil water sustainability of different cropping systems in a dryland agricultural ecosystem. *Agric. Water Manag.* 272, 107834. <https://doi.org/10.1016/j.agwat.2022.107834>.
- Zhang, R., Wang, D., Yang, Z., Seki, K., Singh, M., Wang, L., 2021. Changes in rainfall partitioning and its effect on soil water replenishment after the conversion of croplands into apple orchards on the loess plateau. *Agric. Ecosyst. Environ.* 312, 107342. <https://doi.org/10.1016/j.agee.2021.107342>.
- Zhang, Q., Wang, S., Zhang, Y., Li, H., Liu, P., Wang, R., Wang, X., Li, J., 2021. Effects of subsoiling rotational patterns with residue return systems on soil properties, water use and maize yield on the semiarid loess plateau. *Soil Tillage Res.* 214, 105186. <https://doi.org/10.1016/j.still.2021.105186>.
- Zhao, Y., Wang, Y., Wang, L., Fu, Z., Zhang, X., Cui, B., 2017. Soil-water storage to a depth of 5 m along a 500-km transect on the Chinese loess plateau. *CATENA* 150, 71–78. <https://doi.org/10.1016/j.catena.2016.11.008>.
- Zhu, Y., Cui, Y., 2019. Soil water dynamics and winter wheat performance under precipitation change in the loess tableland region, China. *Agron. J.* 111, 2184–2192. <https://doi.org/10.2134/agronj2018.10.0690>.
- Zhu, Y., Jia, X., Qiao, J., Shao, M., 2019. What is the mass of loess in the loess plateau of China? *Sci. Bull.* 64, 534–539. <https://doi.org/10.1016/j.scib.2019.03.021>.
- Zhu, P., Zhang, G., Wang, H., Zhang, B., Liu, Y., 2021. Soil moisture variations in response to precipitation properties and plant communities on steep gully slope on the loess plateau. *Agric. Water Manag.* 256, 107086. <https://doi.org/10.1016/j.agwat.2021.107086>.